J MATER SCI 41 (2006) 2877–2884

Effect of through-thickness compression on the microstructure of carbon fiber polymer-matrix composites, as studied by electrical resistance measurement

CHIA-KEN LEONG, SHOUKAI WANG, D. D. L. CHUNG*
Composite Materials Research Laboratory, University at Buffalo, State University of New York, Buffalo, NY 14260-4400, USA
E-mail: ddlchung@eng.buffalo.edu

Published online: 17 March 2006

Compression in the through-thickness direction (as in fastening) resulted in reversible and irreversible changes in the microstructure of continuous carbon fiber epoxy-matrix composites, as shown by electrical resistance measurement during dynamic compression. The extent of fiber-fiber contact across the interlaminar interface was increased, with partial irreversibility even at a low stress amplitude of 1 MPa. Within a lamina, fiber squeezing in the through-thickness direction and fiber spreading in the transverse direction occurred upon fastening compression, with partial irreversibility at a stress amplitude of 100 MPa or above. For a single laminae beyond 400 MPa, the lessening of fiber squeezing in the through-thickness direction during unloading dominated over the fiber spreading in the transverse direction during loading.

1. Introduction

Continuous carbon fiber epoxy-matrix composites are important for lightweight structures. Fastening is a common method of joining composite components. In the case of composite laminates, fastening involves compression in the direction perpendicular to the laminae, i.e., through-thickness compression. The effect of fastening on the microstructure of composite laminates is of current aircraft safety concern, due to the 2001 Airbus accident in New York. The accident involved detachment of the tail from the body of the aircraft [1]. This accident and the general aging of aircraft have added impetus to the use of nondestructive methods to evaluate the damage in composite materials. In contrast to metal components, composite components that are identically manufactured tend to differ slightly in the amounts, types and locations of various types of flaws, such as fiber waviness, fiber-matrix debonding, delamination, and the precursor of delamination cracks. Thus, for the purpose of hazard mitigation and timely repair, structural health monitoring is needed for the composite components of aircraft and other strategic structures.

Damage in carbon fiber polymer-matrix composites can be monitored nondestructively by ultrasonic inspection. This technique is limited to the detection of well-defined cracks of diameter at least about 1 mm, typically at least about 1 cm. The size limit depends on the wavelength of the ultrasonic wave and the size of the test probe. A more recent method involves the embedment of fiber-optic sensors in the composite, but this method is intrusive, suffers from poor maintainability, and tends to cause mechanical property loss (partly due to the distortion of the carbon fibers around the fiber-optic sensors).

Due to the high electrical conductivity of carbon fibers compared to the polymer matrix (typically epoxy), the composite is conductive, such that the conductivity is sensitive to the extent of fiber-fiber contact in the transverse and through-thickness directions. A decrease in the extent of fiber-fiber contact along the through-thickness direction (as in the case of delamination) obviously decreases the through-thickness conductivity. A decrease in the extent of fiber-fiber contact along the transverse direction (i.e., direction perpendicular to the fibers in the plane of a lamina) similarly decreases the transverse conductivity.

*Author to whom all correspondence should be addressed.
0022-2461
DOI: 10.1007/s10853-005-5121-7

Fiber damage, which tends to occur only in locations of heavy damage of the composite, will obviously decrease the conductivity in the fiber direction of the composite. Thus, electrical conductivity measurement in one or more directions of a composite provides a nondestructive method of monitoring damage or microstructural changes [2–27]. Damage is associated with mechanical property degradation, whereas a microstructural change is not necessarily associated with such degradation. This method is also advantageous in its fast response, equipment simplicity and applicability to large structural components.

Considerable prior attention has been given to studying the effect of tension in the fiber direction of a composite on the microstructure of the composite [2–13]. This is because the fiber direction is the strong direction of the composite and the composite is stronger under tension than compression in this direction. In contrast, this paper is focused on the effect of compression in the through-thickness direction, due to its relevance to fastening.

This paper uses DC electrical resistance to monitor the effect of repeated compression in the through-thickness direction at various stress amplitudes (equivalent to repeated fastening and unfastening at various loads) on the microstructure of the interlaminar interface (i.e., the interface between adjacent laminae) and on that within a lamina. The effect of through-thickness compression on the microstructure of the interlaminar interface was studied by measuring the contact electrical resistivity of the interface, as previously performed during variation in temperature or shear stress [28–30]. The effect of through-thickness compression on the microstructure of a lamina was studied in this work by measuring the volume resistance of a lamina in both the longitudinal and transverse directions. This paper is aimed at identifying the extents and conditions of stress-induced microstructural changes, particularly those that are too subtle or reversible for microscopic observation to be feasible. Such knowledge is valuable for understanding the mechanical behavior and damage evolution. This paper is not aimed at damage monitoring.

2. Experimental methods

The composites were made from a unidirectional carbon fiber epoxy-matrix prepreg (Cape Composites Inc., San Diego, CA). The properties of the prepreg constituents are shown in Table I.

TABLE I Carbon fiber and epoxy matrix properties (according to Cape Composites Inc., San Diego, CA)

Fortafil 555 continuous carbon fiber	
Diameter	6.2 μm
Density	1800 kg/m^3
Tensile modulus	231 GPa
Tensile strength	3.80 GPa
Cape C2002 epoxy	
Processing temperature	121°C
Flexural modulus	99.9 GPa
Flexural strength	1.17 MPa
T_g	129°C
Density	1150 kg/m^3

For the purpose of determining the mechanical properties of a composite made from the prepreg of Table I, the longitudinal tensile properties of a unidirectional eight-lamina composite made using the prepreg of Table I and the curing conditions mentioned below were determined by tensile testing (up to failure) and the use of a strain gage adhered to a side of the specimen. Stress was provided by a hydraulic mechanical testing system (MTS 810, MTS Systems Corp., Marblehead, MA). The specimen was of size 177 × 10 × 1 mm. A glass fiber reinforced epoxy end-tab of length 32 mm was applied by adhesion to each end of the specimen, so the specimen length excluding the end-tabs was 113 mm. Three specimens were tested. This testing showed that the tensile strength was 2.03 ± 0.08 GPa and the tensile modulus was 148 ± 7 GPa. The fiber volume fraction was 0.58, as shown by density measurement. Based on the Rule of Mixtures and ignoring the matrix contribution, the calculated tensile strength was 2.20 GPa and the calculated tensile modulus was 134 GPa. Thus, there is reasonable consistency between the measured and calculated values for both strength and modulus.

For measuring the contact resistivity of the interlaminar interface, two laminae of prepreg in the form of strips crossing one another, with one strip on top of the other (Fig. 1), were fabricated into a composite at the overlapping region (ranging from 3 × 3 to 6 × 6 mm) of the two laminae by applying pressure and heat to the overlapping region (without a mold). The pressure was provided by weights. A glass fiber epoxy-matrix composite spacer was placed between the weight and the junction (the overlapping region of the two strips). The heat was provided by a Carver hot press. A Watlow model 981C-10CA-ARRR temperature controller was used to control the temperature and the ramping rate. Each of the specimens was put between the two heating platens of the hot press and heated linearly up to 121 ± 2°C at the rate of 2°C/min. Then it was cured at

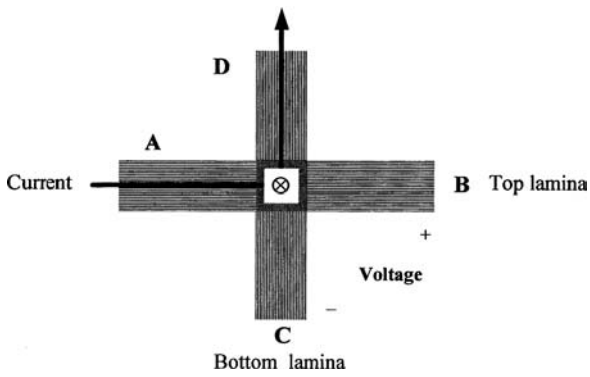

Figure 1 Composite configuration for measuring the contact electrical resistivity of the interlaminar interface. A and D are current contacts; B and C are voltage contacts.

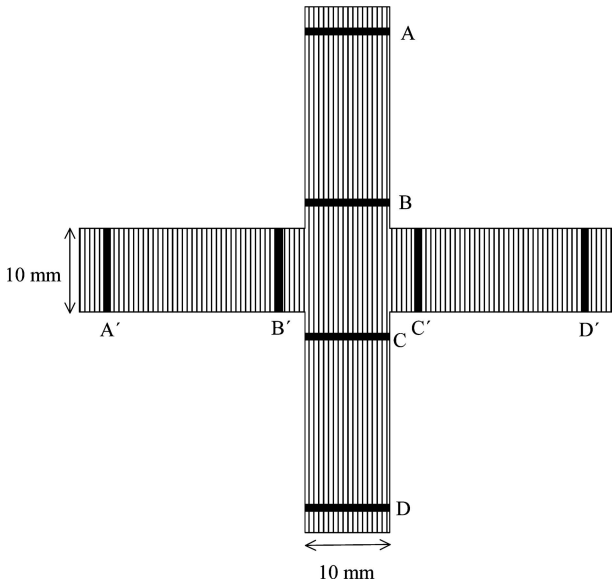

Figure 2 Composite configuration for measuring the volume electrical resistance of a single lamina in both the longitudinal and transverse directions. A and D are current contacts, while B and C are voltage contacts, all for measuring the longitudinal volume resistance. A′ and D′ are current contacts, while B′ and C′ are voltage contacts, all for measuring the transverse volume resistance. All dimensions are in mm. The distance between A and D and that between A′ and D′ are 80 mm. The distance between B and C and that between B′ and C′ are 20 mm.

that temperature for 3 h and subsequently furnace cooled to room temperature.

For measuring the volume resistance of a lamina in both longitudinal and transverse directions, a single lamina of prepreg was cut into the shape of a cross, as shown in Fig. 2. After the cutting, the composite was cured by hot pressing as described above in relation to Fig. 1.

In this work, only one lamina was used for each fiber orientation, because of the aim of studying the interlaminar interface and of fundamental investigation of the microstructural effects of through-thickness compression within a lamina. Study of the overall behavior of a laminate with a substantial number of laminae is not the goal of this work.

In both Figs 1 and 2 the resistance was measured by using the four-probe method. In this method, the outer two contacts are for passing the current, while the inner two contacts are for measuring the voltage. In Fig. 1 the current goes from A to D by first going from A along the top lamina, crossing the interlaminar interface and then going along the bottom lamina toward D. The voltage between B and C, divided by this current, gives the contact resistance of the interlaminar interface. This contact resistance, multiplied by the interface area (i.e., area of the square junction) gives the contact resistivity. In Fig. 2, contacts A, B, C and D (A and D for current, B and C for voltage) are for measuring the longitudinal volume resistance, while contacts A′, B′, C′ and D′ are for measuring the transverse volume resistance. A Keithley 2002 multimeter (Keithley Instruments Inc., Cleveland, OH) was used for the resistance measurement. All electrical contacts were in the form of silver paint in conjunction with copper wire. Each contact in Fig. 1 was wound around the perimeter of the specimen. Each contact in Fig. 2 was applied only on the top surface of the lamina, as the bottom surface was in contact with release paper, which served to support the fragile specimen.

A dynamic compressive stress was applied on the square region in the middle of Figs 1 and 2 via a steel piston (electrically insulated with a Mylar film) of size equal to the square region. The stress was provided by a screw-action mechanical testing system (Sintech 2/D, MTS Systems Corp., Elden Prairie, MN) in case of Fig. 1 and a hydraulic mechanical testing system (MTS 810, MTS Systems Corp., Marblehead, MA) in case of Fig. 2. Simultaneously, the resistance was measured. In the case of Fig. 2, the longitudinal and transverse resistances were measured simultaneously.

Because the compressive strain in Fig. 2 was not measured, the volume resistivity was not determined. Nevertheless, the measured volume resistance gives valuable information.

3. Results and discussion

3.1. Effect on the microstructure of the interlaminar interface

Fig. 3 shows the variation of the contact resistivity with stress during compressive stress cycling to various maximum stresses up to 4 MPa. The composite was made at a curing pressure of 0.43 MPa. The contact resistivity decreased quite reversibly upon loading, due to the increased contact between fibers of adjacent laminae. (Microscopic observation of the change in the degree of contact between fibers of adjacent laminae is difficult, due to the reversibility and subtle nature of the change.) However, the resistivity decrease was not completely reversible. The greater the stress, the more the contact resistivity decreased. Although Fig. 3 shows results at maximum stresses up to 4 MPa, similar results were obtained up to 26 MPa.

The upper envelope of the resistivity variation in Fig. 3 decreased gradually cycle by cycle. This means that the resistivity decrease upon loading was not totally reversible. The partial irreversibility means that the increase in the extent of contact between fibers of adjacent laminae upon loading is not completely reversible.

Stress cycling at a fixed maximum stress of 20 MPa for 14 cycles (Fig. 4) showed that both the upper and lower envelopes of the resistivity decreased irreversibly and gradually leveled off as cycling progressed, while the reversible effect within a cycle was essentially not affected. The irreversible effect is an irreversible microstructural change of the interlaminar interface. This change may be the precursor of damage. It was most significant in the first two cycles and subsequent incremental change diminished as cycling progressed.

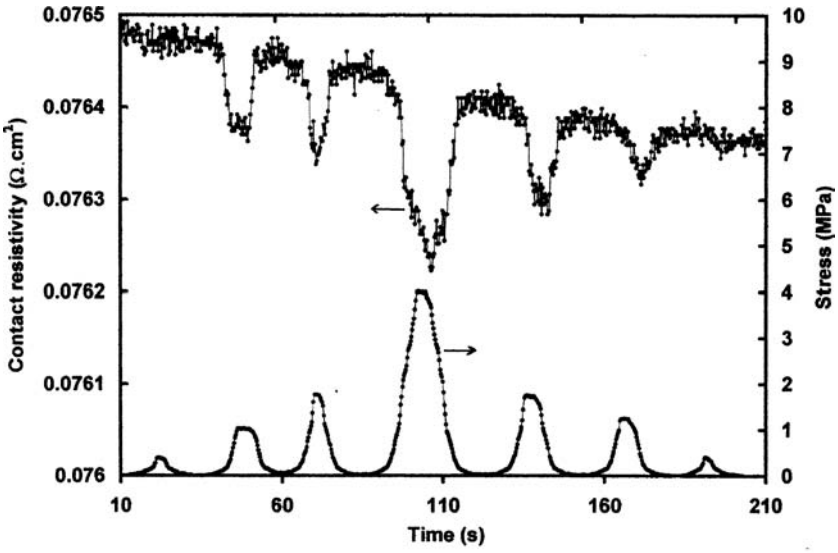

Figure 3 Variation of the contact electrical resistivity with time and of the stress with time during stress cycling to different stress amplitudes up to 4 MPa. The specimen configuration is that in Fig. 1.

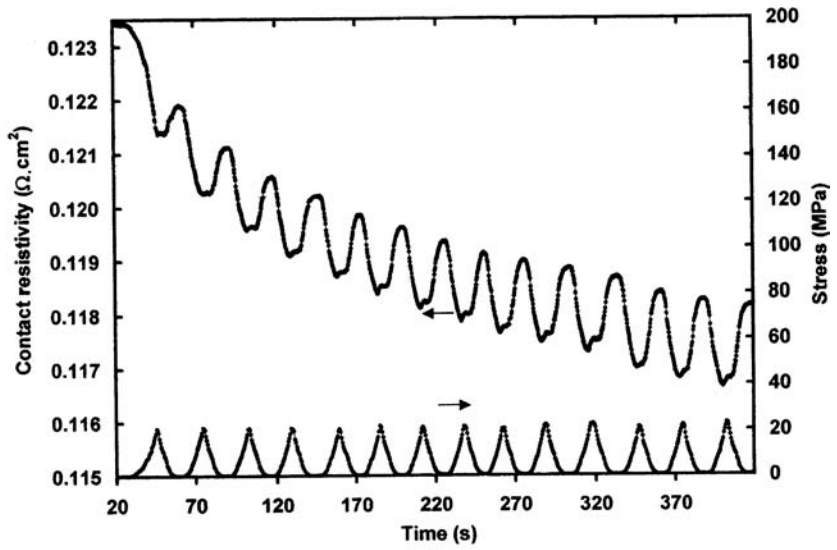

Figure 4 Variation of the contact resistivity with time and of the stress with time during stress cycling at a constant stress amplitude of 20 MPa. The specimen configuration is that in Fig. 1.

Comparison of Figs 3 and 4 suggests that the irreversible decrease in contact resistivity was more severe when the stress was higher, as expected.

3.2. Effect on the microstructure of a lamina

Fig. 5 shows the variation of the longitudinal resistance during dynamic compression at progressively increasing maximum stresses up to fracture, such that three stress cycles were conducted at each value of the maximum stress. The resistance decreased upon compressive loading, in spite of the expected accompanying decrease in thickness (not measured) tending to cause the resistance to increase. The resistance decrease is thus not due to the change in thickness. It is attributed to fiber squeezing (i.e., increase in the extent of fiber-fiber contact, as expected upon compression) in the through-thickness direction and the consequent decrease in the through-thickness volume resistivity (not measured). Microscopic evidence of the fiber squeezing was not obtained, due to the difficulty of performing microscopy during compression and the subtleness of the effect. A decrease in the through-thickness resistivity is expected to cause the longitudinal resistivity to decrease, due to the increased chance of the current to detour from one fiber to an adjacent fiber. This detour would enhance the longitudinal conductivity in the usual case that some fibers are imperfect. The effect is reversible, as shown upon unloading.

As the maximum stress increased, the amplitude of resistance change increased, as expected. Among the three

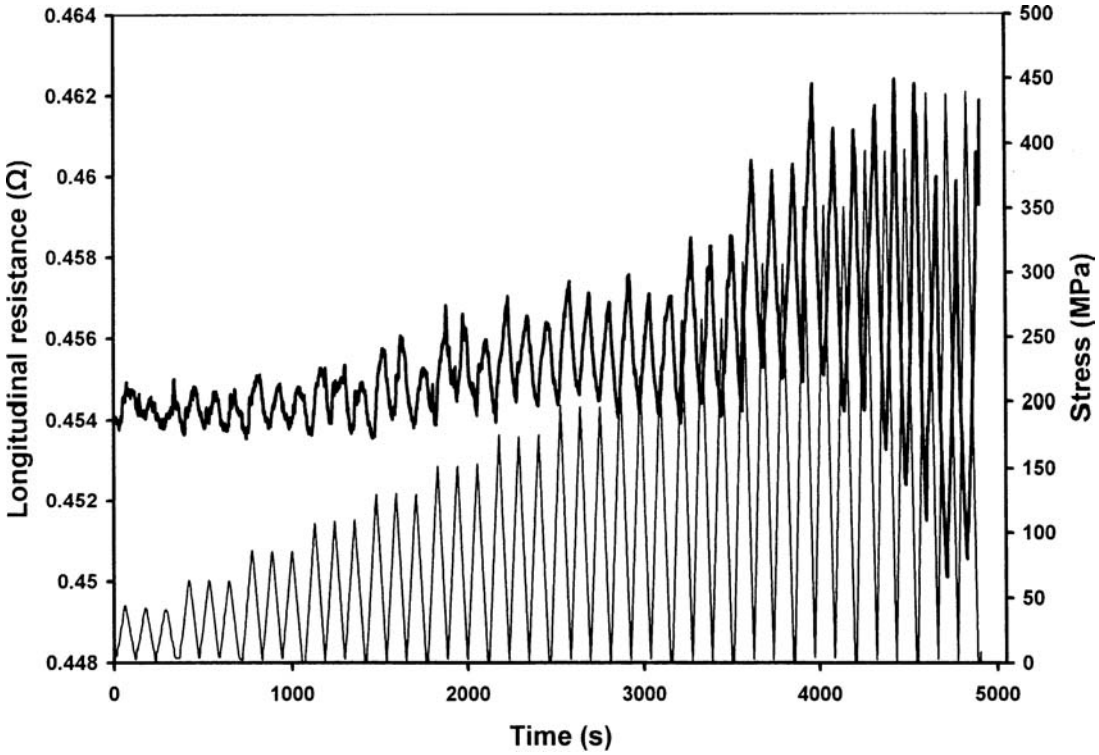

Figure 5 Variation of the longitudinal volume electrical resistance with time (thick curve) and of the stress with time (thin curve) during stress cycling at progressively increasing stress amplitudes up to 450 MPa. Fracture was observed at the end of this test.

cycles at the same maximum stress, the amplitude of resistance change was higher in the first cycle than the subsequent two cycles (except when the maximum stress was 400 MPa or above). At any particular maximum stress, the resistance decrease during loading in the first cycle was followed upon subsequent unloading by a resistance increase such that the resistance after unloading was substantially higher than that before the first loading at this maximum stress. This indicates an irreversible microstructural change (possibly a form of damage) occurring during unloading in the first cycle at this maximum stress. In the subsequent two cycles at this maximum stress, no further irreversible microstructural change was inflicted, as indicated by the absence of additional resistance increase during unloading in each of these cycles. The irreversible microstructural change was of a type that caused the longitudinal resistance to increase. It may relate to a minor degree of fiber damage, since fiber damage is expected to increase the longitudinal resistance. As expected, a greater extent of microstructural change occurred when a maximum stress was experienced for the first time.

Fig. 6 shows the corresponding results on the transverse volume resistance. At maximum stresses up to 310 MPa, the resistance increased upon loading in every cycle. This is due to fiber spreading (i.e., increase of the average distance between adjacent fibers in the transverse direction), as expected. This effect is largely reversible. It is less reversible for the first cycle than the subsequent two cycles at the same maximum stress. Moreover, the amplitude of resistance change was larger for the first cycle than the subsequent two cycles, due to more fiber spreading when a maximum stress was experienced for the first time. Microscopic evidence of the fiber spreading was not obtained, due to the difficulty of performing microscopy during compression and the subtleness of the effect.

During unloading, the resistance decreased. Upon subsequent loading, the resistance continued to decrease, as shown in Fig. 7, which is a magnified view of the low stress portion of Fig. 6. This continued decrease in resistance is due to the increased extent of fiber-fiber contact in the through-thickness direction. After the reloading had reached an intermediate level, the resistance started to increase, due to fiber spreading. In other words, there were two microstructural effects, i.e., fiber spreading in the transverse direction and fiber squeezing in the through-thickness direction. Fiber spreading was the dominant phenomenon, but both phenomena occurred in each stress cycle.

At maximum stresses above 310 MPa, the resistance started to increase when unloading was near completion, thereby resulting in a spike at zero load. This effect is due to the lessening of fiber squeezing in the through-thickness direction. At maximum stresses above 350 MPa, this spike was the dominant effect in a cycle, i.e., the phenomenon associated with the lessening of fiber squeezing in the through-thickness direction overshadowed the phenomenon associated with fiber spreading in the transverse direction, probably because the fiber spreading had

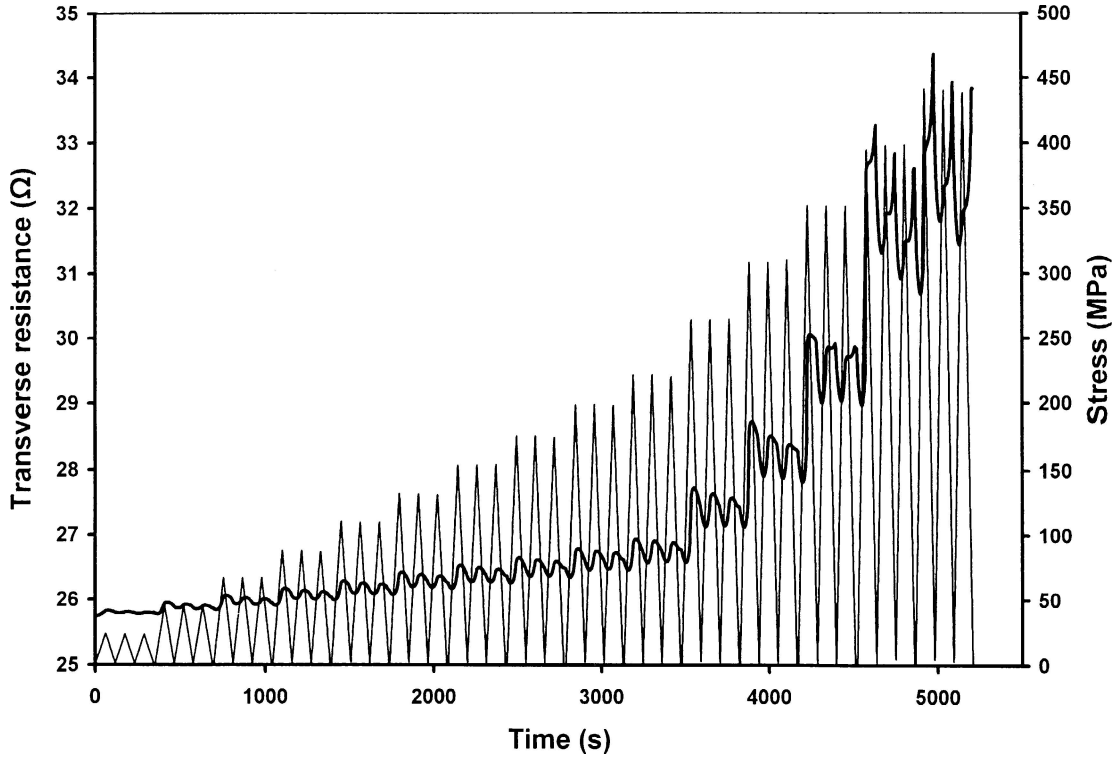

Figure 6 Variation of the transverse volume electrical resistance with time (thick curve) and of the stress with time (thin curve) during stress cycling at progressively increasing stress amplitudes up to 450 MPa. Fracture was observed at the end of this test.

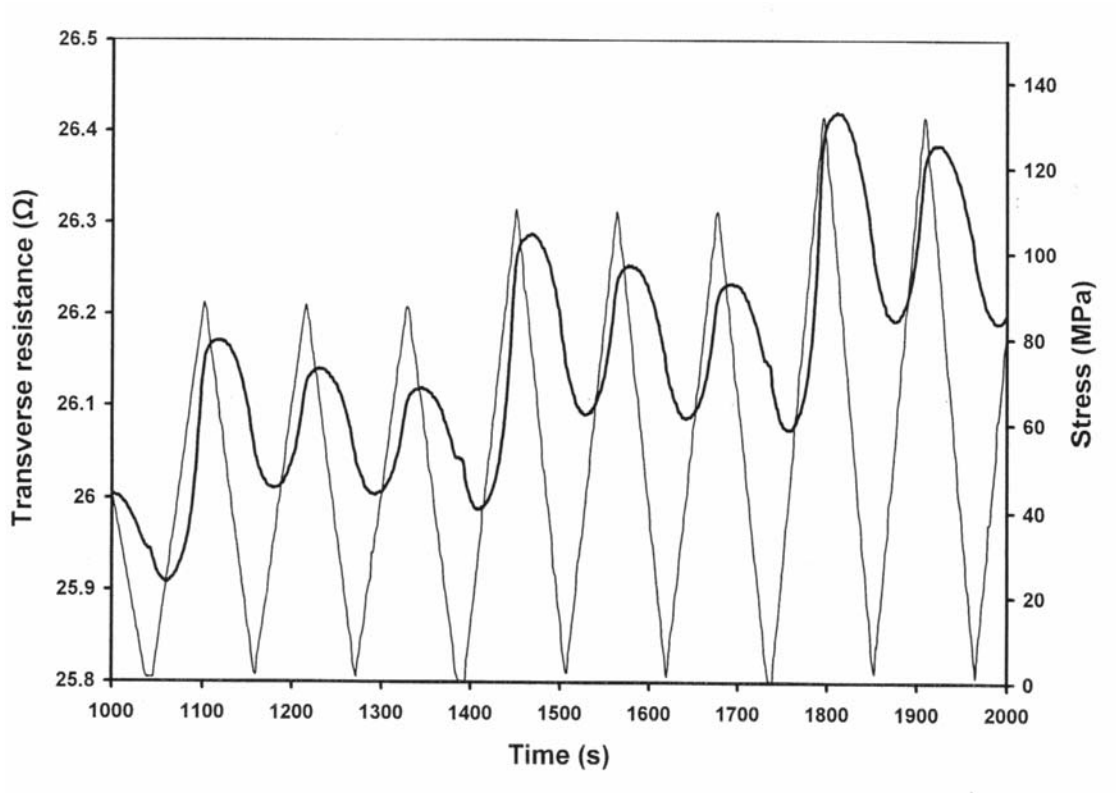

Figure 7 Magnified view of a part of Fig. 6.

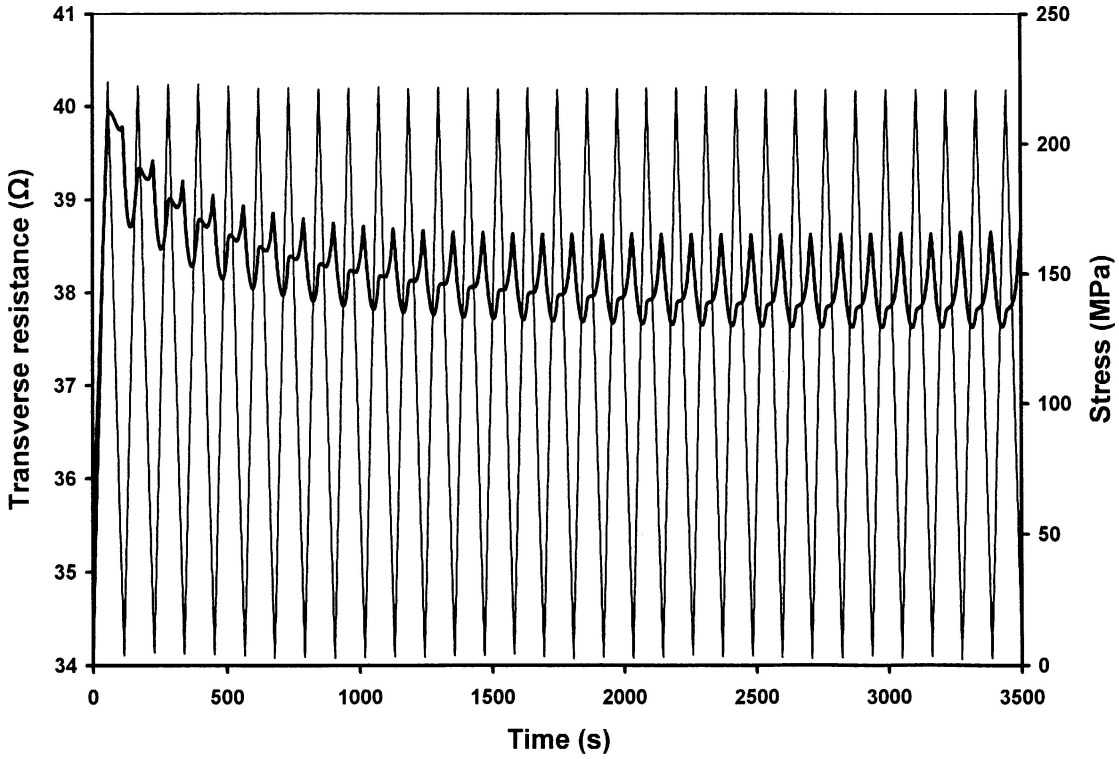

Figure 8 Variation of the transverse volume electrical resistance with time (thick curve) and of the stress with time (thin curve) during stress cycling at a fixed amplitude. Fracture was not observed.

reached its limit. In other words, fiber spreading was the dominant effect at maximum stresses up to 350 MPa, but the lessening of fiber squeezing in the through-thickness direction was the dominant effect at maximum stresses above 350 MPa.

The change in the dominant effect from fiber spreading in the transverse direction to the lessening of fiber squeezing in the through-thickness direction was also observed from the transverse resistance upon stress cycling at a fixed low maximum stress of 220 MPa, as shown in Fig. 8. As cycling progressed, the phenomenon associated with the lessening of fiber squeezing in the through-thickness direction became more and more dominant.

Fig. 6 also shows that the baseline transverse resistance increased as the maximum stress increased. The increase was gradual at maximum stresses up to 230 MPa, but was increasingly abrupt as the maximum stress increased beyond 230 MPa. This baseline increase is probably due to damage in the form of minor matrix cracks between adjacent fibers.

It should be noted that the maximum stresses in this section are much higher than those in the last section. This means that the microstructure of the interlaminar interface required much less stress in order for it to be changed than the microstructure within a lamina, as expected.

4. Conclusion

Compression in the through-thickness direction (as in fastening) of a carbon fiber epoxy-matrix composite caused the extent of fiber-fiber contact across the interlaminar interface to increase, as shown by decrease in the contact resistivity of this interface. The effect was not totally reversible, even at a small stress amplitude of 1 MPa.

For a single lamina, this compression caused fiber squeezing in the through-thickness direction, as shown by decrease in the longitudinal volume resistance. Accompanying this effect was fiber spreading in the transverse direction, as shown by increase in the transverse volume resistance. Both effects were reversible, though slight and partial irreversibility was observed at the first experience of a maximum stress of 100 MPa or above.

For a single lamina, as the maximum stress increased to 400 MPa, the lessening of fiber squeezing in the through-thickness direction during unloading started to dominate over the fiber spreading in the transverse direction during loading, as shown by the transverse volume resistance increasing upon unloading starting to dominate over the competing phenomenon in which this resistance increased upon loading. This is because of the fiber spreading approaching its limit as the maximum stress increased.

References

1. Eighth Update on NTSB Investigation into Crash of American Airlines Flight 587, NTSB Advisory, National Transportation Safety Board, Washington, DC 20594, June 4, 2002. http://www.ntsb.gov/pressrel/2002/020604.htm.
2. X. WANG and D. D. L. CHUNG, *Smart Mater. Struct.* **5** (1996) 796.
3. *Idem., ibid.* **6** (1997) 504.

4. *Idem., Compos. Part B-Eng.* **29B**(1) (1998) 63.
5. X. WANG, X. FU and D. D. L. CHUNG, *J. Mater. Res.* **13**(11) (1998) 3081.
6. X. WANG and D. D. L. CHUNG, *ibid.* **14**(11) (1999) 4224.
7. S. WANG and D. D .L. CHUNG, *Polym. Comp.* **21**(1) (2000) 13.
8. K. SHULTE and CH. BARON, *Comp. Sci. Technol.* **36** (1989) 63.
9. M. KUPKE, K. SHULTE and R. SCHULER, *ibid.* **61** (2001) 837.
10. A. TODOROKI, *ibid.* **61** (2001) 1871.
11. J. C. ABRY, Y. K. CHOI, A. CHATEAUMINOIS, B. DALLOZ, G. GIRAUD and M. SALVIA, *ibid.* **61**(6) (2001) 855.
12. Z. XIA, T. OKABE, J. B. PARK, W. A. CURTIN and N. TAKEDA, *ibid.* **63**(10) (2003) 1411.
13. N. ANGELIDIS, C. Y. WEI and P. E. IRVING, *Compos. Part A-Appl. S.* **35**(10) (2004) 1135.
14. X. WANG, S. WANG and D. D. L. CHUNG, *J. Mater. Sci.* **34**(11) (1999) 2703.
15. S. WANG and D. D. L. CHUNG, *ibid.* **35**(1) (2000) 91.
16. X. WANG and D. D. L. CHUNG, *Compos. Interf.* **5**(3) (1998) 191.
17. I. WEBER and P. SCHWARTZ, *Compos. Sci. Technol.* **61**(6) (2001) 849.
18. J. C. ABRY, S. BOCHARD, A. CHATEAUMINOIS, M. SALVIA and G. GIRAUD, *ibid.* **59**(6) (1999) 925.
19. N. ANGELIDIS, N. KHEMIRI and P. E. IRVING, *Smart Mater. Struct.* **14** (2005) 147.
20. O. CEYSSON, M. SALVIA and L. VINCENT, *Scripta Mater.* **34**(8) (1996) 1273.
21. Y.-W. CHU and Y.-J. YUM, Proceedings – KORUS 2001, The 5th Korea-Russia International Symposium on Science and Technology, Section 5—Mechanics and Automotive Engineering (2001) p. 240.
22. P. E. IRVING and C. THIAGARAJAN, *Smart Mater. Struct.* **7** (1998) 456.
23. A. S. KADDOUR, A. R. AL-SALEHI, S. T. S. AL-HASSANI and M. J. HINTON, *Compos. Sci. Technol.* **51**(3) (1994) 377.
24. L. C. MASSON and P. E. IRVING, Proceedings of SPIE, 5th European Conference on Smart Structures and Materials **4073** (2000) 182.
25. N. MUTO, H. YANAGIDA, T. NAKATSUJI, M. SUGITA, Y. OHTSUKA and Y. ARAI, *Smart Mater. Struct.* **1** (1992) 324.
26. R. PRABHAKARAN, *Exp. Techniques* **14**(1) (1990) 16.
27. A. TODOROKI, Y. TANAKA and Y. SHIMAMURA, *Compos. Sci. Technol.* **64**(5) (2004) 749.
28. S. WANG and D. D. L. CHUNG, *Comp. Interf.* **6**(6) (1999) 497.
29. *Idem., ibid.* **6**(6) (1999) 507.
30. *Idem., Polym. Polym. Comp.* **9**(2) (2001) 135.

Received 30 March 2004
and accepted 7 July 2005